BIOCHEMISTRY
including biophysical chemistry & molecular biology

Article

pubs.acs.org/biochemistry

Binding Rate Constants Reveal Distinct Features of Disordered Protein Domains

Jakob Dogan,*,† Josefin Jonasson, Eva Andersson, and Per Jemth*

Department of Medical Biochemistry and Microbiology, Uppsala University, BMC Box 582, SE-75123 Uppsala, Sweden

Supporting Information

ABSTRACT: Intrinsically disordered proteins (IDPs) are abundant in the proteome and involved in key cellular functions. However, experimental data about the binding kinetics of IDPs as a function of different environmental conditions are scarce. We have performed an extensive characterization of the ionic strength dependence of the interaction between the molten globular nuclear co-activator binding domain (NCBD) of CREB binding protein and five different protein ligands, including the intrinsically disordered activation domain of p160 transcriptional co-activators (SRC1, TIF2, ACTR), the p53 transactivation domain, and the folded pointed domain (PNT) of transcription factor ETS-2. Direct comparisons of the binding rate constants under identical conditions show that the association rate constant, k_{on}, for interactions between NCBD and disordered protein domains is high at low salt concentrations (90−350 × 10^6 M^{-1} s^{-1} at 4 °C) but is reduced significantly (10−30-fold) with an increasing ionic strength and reaches a plateau around physiological ionic strength. In contrast, the k_{on} for the interaction between NCBD and the folded PNT domain is only 7 × 10^6 M^{-1} s^{-1} (4 °C and low salt) and displays weak ionic strength dependence, which could reflect a distinctly different association that relies less on electrostatic interactions. Furthermore, the basal rate constant (in the absence of electrostatic interactions) is high for the NCBD interactions, exceeding those typically observed for folded proteins. One likely interpretation is that disordered proteins have a large number of possible collisions leading to a productive on-pathway encounter complex, while folded proteins are more restricted in terms of orientation. Our results highlight the importance of electrostatic interactions in binding involving IDPs and emphasize the significance of including ionic strength as a factor in studies that compare the binding properties of IDPs to those of ordered proteins.

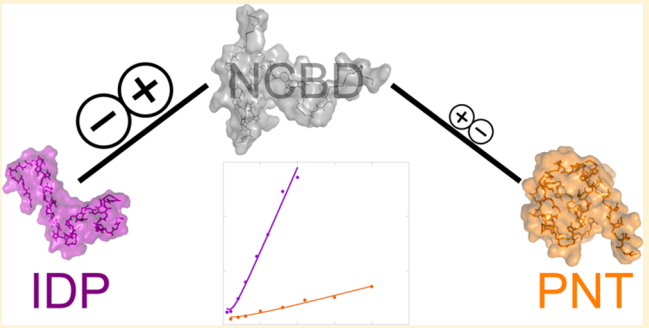

Intrinsically disordered proteins (IDPs) have been shown to play crucial roles in processes such as cellular signaling, transcription, and cell-cycle control.[1] IDPs are not able to fold into homogeneous well-defined globular three-dimensional structures but instead form a heterogeneous ensemble of rapidly interconverting conformations, which often but not always adopt an ordered structure upon binding to their targets. They are abundant in the proteome and have also been shown to be associated with various diseases.[2] It has been proposed that IDPs have advantages with regard to ligand binding, including a greater possibility of modulating the rate constants (e.g., higher k_{on} and k_{off} values) to achieve optimal affinity.[3] Indeed, one important difference between globular and disordered proteins is that the latter contain less hydrophobic and more charged and hydrophilic amino acid side chains.[4] One implication of this property would be that charges play an important role in protein−protein interactions involving IDPs. However, despite the significant attention IDPs now receive in the context of protein−protein interactions, there are few studies that have investigated the binding kinetics of IDPs (see Table 1 of refs 5 and 6), and even fewer studies that have addressed the role of electrostatics in kinetics.[7,8] Previous studies, in which published data sets were used to compare the kinetics of binding of IDPs to folded proteins, concluded that differences in both the association (k_{on}) and dissociation (k_{off}) rate constants could exist.[7,9] However, data from such tabulations were collected under different conditions (pH, temperature, and ionic strength), which can greatly affect the rate constants and jeopardize the conclusions.[5] Thus, there are several remaining questions regarding the binding reactions of IDPs: are there general differences in binding rate constants, binding mechanism, and in the electrostatic contribution to binding between IDP and globular domains? To shed light on these issues and facilitate a direct comparison between IDPs and folded domains, we have in this study investigated the binding kinetics for one protein domain with different binding partners (folded and disordered) under similar conditions.

Often, protein−protein interaction domains have more than one binding partner. The molten globular nuclear co-activator binding domain (NCBD) of the transcriptional co-activator CREB binding protein (CBP)[1,10] is such an interaction domain

Received: May 13, 2015
Revised: July 3, 2015
Published: July 8, 2015

DOI: 10.1021/acs.biochem.5b00520
Biochemistry 2015, 54, 4741−4750

with several interaction partners. Importantly, the interaction partners include both disordered and folded protein domains, for example, the disordered activation domain found in each of the three p160 transcriptional co-activators (NCOA1–NCOA3) and denoted SRC1, TIF2, and ACTR, respectively,[11] the disordered transactivation domain of p53 (p53TAD),[12,13] the folded pointed domain (PNT) of transcription factor ETS-2,[14,15] and the IRF association domain of IRF-3 (IRF-3)[14,16] (Figure 1). In particular, the interaction between NCBD and

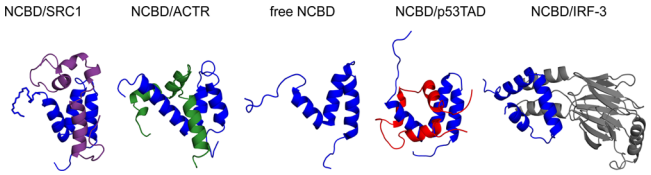

Figure 1. Three-dimensional structure of free state NCBD (PDB entry 2KKJ), flanked by structures of NCBD complexes [PDB entries 2C52 (NCBD/SRC1), 1KBH (NCBD/ACTR), 2L14 (NCBD/p53TAD), and 1ZOQ (NCBD/IRF-3)]. NCBD is colored blue in all five panels. The figures were generated using PyMol (www.pymol.org).

ACTR has been previously characterized in great detail with regard to structure and dynamics,[14,17−20] kinetic binding mechanism,[21] and formation of structure along the coupled binding and folding pathway.[22−24] The well-characterized NCBD system is therefore perfectly suited for a comparative study of the kinetics of binding to different ligands.

The binding kinetics for the NCBD interactions were investigated as a function of ionic strength to five of the binding partners, which allowed us to assess the role of electrostatic interactions, and the binding mechanisms in the case of three coupled binding and folding reactions. We demonstrate that similarities for some of the interactions exist, in terms of binding mechanisms but also the magnitude of rate constants. However, there are also distinct differences between the NCBD ligands, which are presented and discussed in the context of our current understanding.

EXPERIMENTAL PROCEDURES

Protein Expression and Purification. The DNA sequences of the following human proteins were inserted into a modified pRSET vector (Invitrogen): the activation domain of the three p160 transcriptional co-activators; SRC1 (920–970), TIF2 (1071–1110), and ACTR (1018–1088), NCBD of CBP (2058–2116), the PNT domain of transcription factor ETS-2 (four variants; 60–170, 60–174, 60–195, and 76–170), the transactivation domain of p53 (13–61) (p53TAD), and the IRF association domain of IRF-3 (173–394). All of the proteins were expressed in fusion with an N-terminal His_6-tagged lipoyl protein domain followed by a thrombin cleavage site. *Escherichia coli* BL21(DE3) plysS cells (Invitrogen) were grown to an OD_{600} of 0.7–0.9 at 37 °C, after which protein expression was induced using 1 mM isopropyl β-D-thiogalactopyranoside at 18 °C overnight. Cells were harvested by centrifugation, resuspended in 30 mM Tris-HCl (pH 8.0) and 200 mM sodium chloride (1–2 mM reducing agent added for IRF-3 and PNT), and lysed by ultrasonication. After a second centrifugation, the lysate was sterile filtered and the expressed protein was purified by nickel affinity chromatography [washed with 30 mM Tris-HCl (pH 8.0), 500 mM sodium chloride, and 20 mM imidazole and eluted with 250 mM imidazole (pH 7.9) and 500 mM sodium chloride], followed by dialysis against 20 mM Tris-HCl (pH 8.0) and 100 mM sodium chloride and subsequent thrombin cleavage to remove the fusion protein. The protein solution was again loaded onto a nickel affinity column with a serially attached benzamidine column, to remove the fusion protein, impurities, and thrombin. To eliminate any remaining impurities, a C8 reversed phase purification step [standard water/acetonitrile solvents, 0.1% (v/v) trifluoroacetic acid] was conducted for SRC1, TIF2, ACTR, NCBD, and p53TAD, whereas for the PNT domain and IRF-3, this step was replaced with anion exchange chromatography in Tris-HCl buffer at pH 8.0. During the purification of the PNT domain and IRF-3, 0.5–1 mM TCEP was used as a reducing agent. A Trp variant of NCBD ($NCBD_{Y2108W}$) was purified and used in the kinetic binding experiments as detailed in the next section. This variant has been previously shown to have the same properties as the wild-type NCBD ($NCBD_{WT}$).[21] Purity and identity were checked with sodium dodecyl sulfate–polyacrylamide gel electrophoresis and matrix-assisted laser desorption ionization time-of-flight, respectively.

Stopped-Flow Fluorimetry. Measurements were taken using an upgraded SX-17MV stopped-flow spectrometer (Applied Photophysics, Leatherhead, U.K.). All experiments were performed at 277 K in 10 mM MOPS (pH 7.4) or 20 mM sodium phosphate (pH 7.4) buffer, at different ionic strengths adjusted using sodium chloride. For $NCBD_{WT}$/PNT, 0.9 mM dithiothreitol (DTT) was also added to the experimental buffer. For the interactions between NCBD and SRC1, TIF2, and ACTR, the Trp variant $NCBD_{Y2108W}$ was used to obtain a change in fluorescence upon binding. Both PNT and p53TAD contain Trp residues that were used to monitor a change upon binding to $NCBD_{WT}$. Excitation was at 280 nm, and the fluorescence emission was monitored by using a 330 nm band-pass filter for $NCBD_{WT}$/PNT and a 320 nm long-pass filter for the remaining binding interactions. The association rate constants (k_{on}) for $NCBD_{Y2108W}$/SRC1, $NCBD_{Y2108W}$/TIF2, and $NCBD_{Y2108W}$/ACTR were obtained by varying the concentration (0.1–16 μM) of SRC1, TIF2, and ACTR, respectively, with the concentration of $NCBD_{Y2108W}$ held constant at 0.2–1.0 μM. For $NCBD_{WT}$/PNT, the concentration of $NCBD_{WT}$ was varied while the PNT domain concentration was kept constant at 2 μM, to obtain k_{on}. Experimental binding traces for $NCBD_{WT}$/PNT were fitted to a single-exponential equation to obtain k_{obs}. The binding kinetics of $NCBD_{Y2108W}$/TIF2 (Figure S1A of the Supporting Information) and $NCBD_{Y2108W}$/ACTR were biphasic as described previously,[21,22] with a fast phase that showed a linear dependence on TIF2 or ACTR concentration and a slow phase that remained approximately constant with an increasing concentration (Figure S1B of the Supporting Information). The binding kinetics of $NCBD_{Y2108W}$/SRC1 appeared to be monophasic (Figure 3A) with a k_{obs} that displayed a linear concentration dependence (Figure 3C). At an ionic strength of 1 M, an additional kinetic phase, also described previously for $NCBD_{Y2108W}$/ACTR,[21] appeared for all three NCBD/p160 interactions, with a k_{obs} that did not change with an increasing concentration of the varying species (Figure S2 of the Supporting Information). The linearly increasing kinetic phases ($NCBD_{Y2108W}$/SRC1, $NCBD_{Y2108W}$/TIF2, $NCBD_{Y2108W}$/ACTR, and $NCBD_{WT}$/PNT) were analyzed by fitting an equation for a second-order binding[25] to obtain the association rate constant k_{on} at each ionic strength. Data fitting was performed using Kaleidagraph (Synergy Software).

DOI: 10.1021/acs.biochem.5b00520
Biochemistry 2015, 54, 4741–4750

Displacement experiments were performed to determine the dissociation rate constant (k_{off}). This was achieved by challenging a preformed complex of $NCBD_{Y2108W}$/ACTR, $NCBD_{Y2108W}$/SRC1, or $NCBD_{Y2108W}$/TIF2 with an excess of $NCBD_{WT}$ and monitoring the fluorescence change, while for $NCBD_{WT}$/PNT or $NCBD_{WT}$/p53TAD, an excess of SRC1 was used. All experimental traces were monophasic and fitted to a single-exponential equation to obtain k_{obs}, which is equal to k_{off} with an excess of the competitor ($NCBD_{WT}$ or SRC1). It was not possible to determine k_{on} for $NCBD_{WT}$/p53TAD because of elevated observed rate constants, but because we were able to obtain k_{off} in the displacement experiment, we combined isothermal titration calorimetry [to get K_d (see below)] with stopped-flow spectroscopy (to get k_{off}) and calculated k_{on} ($=k_{off}/K_d$) for $NCBD_{WT}$/p53TAD, at the three lowest ionic strengths.

Isothermal Titration Calorimetry (ITC). ITC measurements were performed using an iTC200 calorimeter (Malvern Instruments). The temperature was set to 277 K, and measurements were taken in 10 mM MOPS (pH 7.4), at different ionic strengths, adjusted with sodium chloride. Proteins were dialyzed against the experimental buffer before the ITC measurements were taken. For $NCBD_{WT}$/p53TAD, concentrations of $NCBD_{WT}$ ranging from 0.86 to 2.1 mM were titrated into a 75−190 μM p53TAD solution. Higher protein concentrations were used in the experiments at the higher ionic strength, to compensate for the lower affinity. For $NCBD_{WT}$/IRF-3, $NCBD_{WT}$ at a concentration of 1.4 mM was titrated into a 56 μM IRF-3 solution, at an ionic strength of 0.2 M in presence of 0.8 mM TCEP. We also attempted binding experiments at low ionic strengths, but mixing IRF-3 (in fusion with the lipoyl domain) with NCBD resulted in precipitation. Typically, a titration series consisted of a preliminary 0.4 or 0.5 μL injection followed by 20−23 subsequent 1.7−1.9 μL injections. Data were fitted to a 1:1 binding model using the software provided by the manufacturer.

Stability Measurements. The thermodynamic stability of PNT(60−174) was determined by GdnHCl-induced denaturation monitored by fluorescence using a SLM4800 spectrofluorimeter (OLIS, Inc.). Experiments were conducted at 298 K and in 20 mM MOPS (pH 7.4), 190 mM sodium chloride, and 2 mM DTT. Fluorescence excitation was at 280 nm, and emission spectra were recorded at each GdnHCl concentration (0−7.3 M), while the concentration of the PNT domain was kept constant at 3 μM. Data were fitted to a two-state transition[26] using Kaleidagraph (Synergy Software).

Circular Dichroism (CD) Spectroscopy. Far-UV CD spectra were recorded at 298 K, using a JASCO-810 CD spectropolarimeter, and a 0.1 cm cuvette. Protein concentrations were 20 μM for SRC1 and p53TAD, 30 μM for TIF2, and 10 μM for the PNT domain, in 20 mM sodium phosphate (pH 7.4) and 150 mM sodium chloride. For the PNT domain, 0.7 mM TCEP was included in the buffer.

Calculation of Basal Rate Constants. k_{on} as a function of ionic strength, I, was fit to a Debye−Hückel-like approximation according to eq 1, to calculate the basal rate constant $k_{on,basal}$[27] i.e., in the absence of electrostatic effects

$$\ln k_{on} = \ln k_{on,basal} - \left(\frac{U}{RT}\right)\frac{1}{1+\kappa\alpha} \quad (1)$$

where R is the gas constant, T is the temperature, U is the electrostatic interaction energy, κ is equal to $(2N_A e^2 I/e_0 e_r k_B T)^{1/2}$, where N_A is Avogadro's constant, e is the elementary charge, I is the ionic strength, e_0 is the vacuum permittivity, e_r is the dielectric constant of water, k_B is the Boltzmann constant, and T is the temperature. α is the minimal distance of approach and is set to 6 Å.[8,27]

RESULTS

We investigated the interaction between NCBD and six different protein partners using stopped-flow spectroscopy and ITC. Four of these are intrinsically disordered protein domains, and two are folded globular domains. The activation domain of the p160 co-activators (TIF2 and ACTR)[14,17,28,29] and p53TAD[13,30,31] have been previously shown to be intrinsically disordered. Indeed, the CD spectra of these domains and that of the previously uncharacterized free state SRC1 (Figure 2A) display the characteristics of a disordered protein, in terms of both the magnitude of the signal and the shape of the spectrum. An X-ray structure of the PNT(76−170) domain has recently been determined (PDB entry 4MHV), showing it to be a compact α-helical protein. We determined the stability of the PNT domain using GdnHCl-induced denaturation (Figure 2B). The free energy of unfolding is 5.1 kcal/mol at 298 K, which means that the PNT domain is a relatively stable protein domain. Furthermore, the PNT domain has CD properties typically observed for α-helical

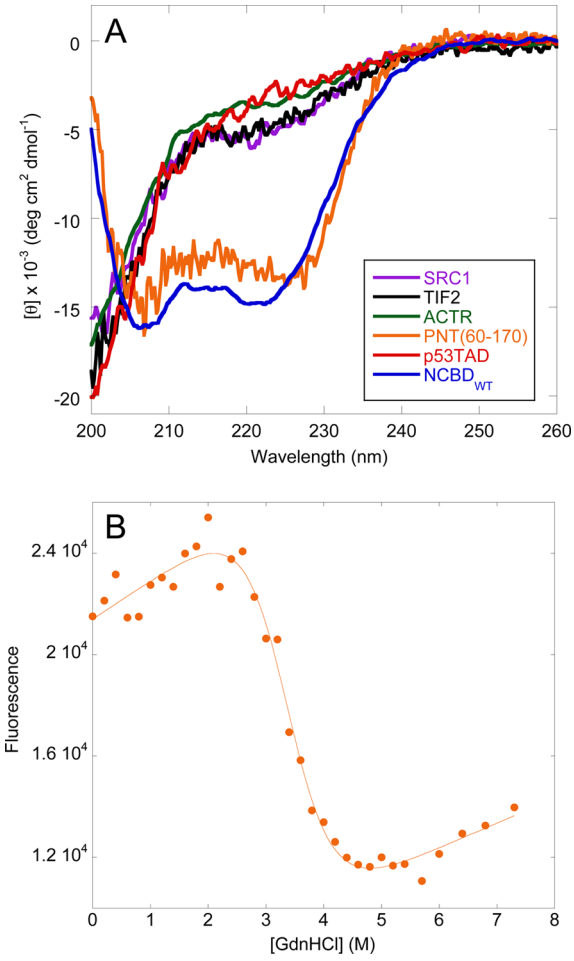

Figure 2. (A) CD spectra of SRC1, TIF2, ACTR NCBD, and the PNT domain of ETS-2(60−170). The CD data for ACTR and NCBD were published previously.[21] (B) Fluorescence-monitored guanidine hydrochloride denaturation of PNT at 298 K.

DOI: 10.1021/acs.biochem.5b00520
Biochemistry 2015, 54, 4741−4750

proteins, in agreement with the crystal structure. The bound IRF-3 structure is a β-sandwich that also includes three α-helices, two of which provide the interaction surface for NCBD.[16] The three NCBD helices observed in the SRC1/ACTR/p53-bound conformation are also formed in the IRF-3 complex; however, their tertiary arrangement is different.[16] Despite these fascinating differences, a biophysical characterization of the interaction between IRF-3 and NCBD has not yet been reported. The binding of these six protein domains (four disordered and two ordered) with NCBD was investigated as detailed below.

Binding Kinetics of NCBD and the p160 Activation Domains. The binding kinetics of NCBD with the activation domains of the three p160 co-activators were measured using stopped-flow fluorimetry. NCBD was mixed with its respective protein ligand and the change in fluorescence upon binding monitored with time. Previous studies of the NCBD/ACTR interaction have shown that the binding kinetics is multiphasic, with at least three kinetic phases.[21,22] The same three kinetic phases were observed for NCBD/TIF2, with similar magnitudes of the three observed rate constants[21] (Figures S1 and S2 of the Supporting Information). For NCBD/SRC1, the slowest kinetic phase was not observed, which, however, is likely due to the lower signal-to-noise ratio in the kinetic traces compared to those of the kinetic traces of NCBD/ACTR and NCBD/TIF2. These results imply that the same binding mechanism is in operation for at least two of the three NCBD/p160 activation domain interactions.

One of the kinetic phases increased linearly with an increasing concentration of SRC1, TIF2, and ACTR and was used to obtain k_{on} (Figure 3C and Figure S1 of the Supporting Information) for each of the five ionic strengths investigated (Figure 4B and Table 1). The k_{on} had a significant ionic strength dependence at lower salt concentrations but rapidly reached a plateau at ~0.2 M (Figure 4B), where the k_{on} for SRC1 and ACTR was ~3×10^7 M^{-1} s^{-1}, whereas the k_{on} for TIF2 was approximately twice as high. The change in k_{on}, when going from a low to a high ionic strength, was around 10−15-fold, indicating the importance of electrostatic interactions in these association reactions (Figure 4B and Table 1). The k_{off} values were also very similar for the three p160 co-activator domains, with values of 1.5, 3.1, and 2.7 s^{-1} for the SRC1, TIF2, and ACTR interactions, respectively, at an ionic strength of 0.2 M (Figure 4A and Table 1).

Binding Kinetics of NCBD and p53TAD. The observed rate constant for the binding of NCBD and p53TAD was at the limit of the stopped-flow instrument, even at the lowest ligand concentrations. However, using a displacement experiment for the stopped flow, we determined the dissociation rate constant k_{off} for $NCBD_{WT}$/p53TAD to be 280 s^{-1} at an ionic strength of 0.04 M. This value is 2 orders of magnitude higher than those obtained for the interactions with the p160 co-activator domains. The large k_{off} precluded a direct measurement of k_{on} for the interaction between NCBD and p53TAD using the stopped-flow technique. We therefore determined k_{on} by measuring the K_d using ITC and then using k_{off} measured in the separate displacement experiment to calculate $k_{on} = k_{off}/K_d$. The K_d value was determined to be 3 μM at an ionic strength of 0.04 M (Figure 5A and Table 1) but increased to ~90 μM at an ionic strength of 0.2 M (Figure 5B and Table 1). A further increase in salt concentration did not significantly affect K_d (Figure 4C). The observed effect of the ionic strength on K_d was found to be almost entirely due to a decreasing k_{on} value.

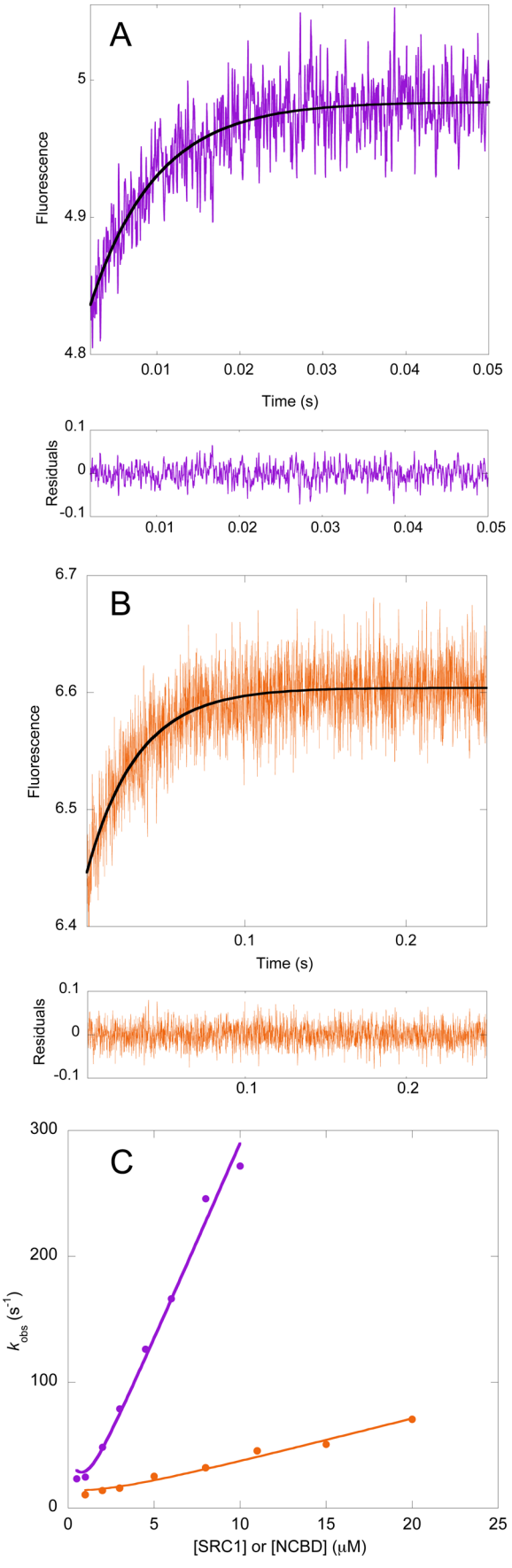

Figure 3. Example of stopped-flow binding traces for the reaction between (A) 1 μM $NCBD_{Y2108W}$ and 4.5 μM SRC1 and (B) 2 μM

DOI: 10.1021/acs.biochem.5b00520
Biochemistry 2015, 54, 4741−4750

Figure 3. continued

PNT and 8 μM $NCBD_{WT}$. The traces were fitted to a single-exponential function to obtain k_{obs} values. (C) k_{obs} as a function of SRC1 (purple, constant $NCBD_{Y2108W}$ concentration) or $NCBD_{WT}$ (orange, constant PNT concentration) concentration. The experiments were performed in 10 mM MOPS (pH 7.4) at an ionic strength of 0.2 M.

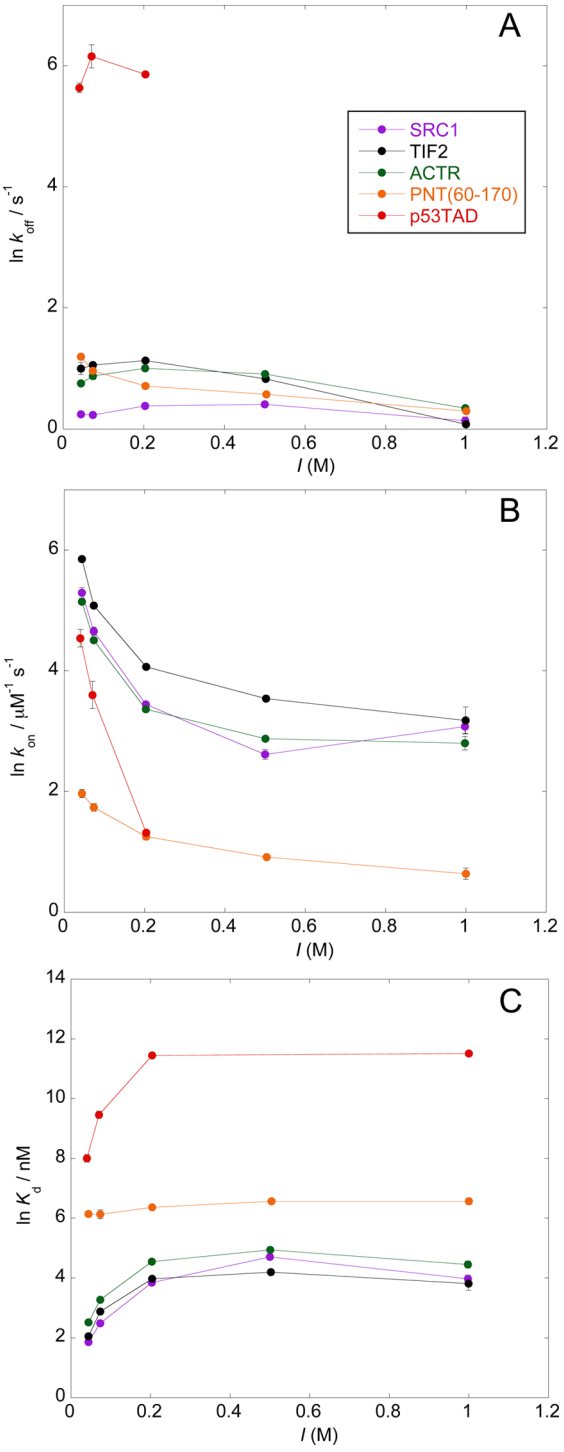

Figure 4. Ionic strength dependence of (A) k_{off}, (B) k_{on}, and (C) K_d. Experiments were conducted at 277 K and in 10 mM MOPS (pH 7.4), with the ionic strength adjusted using sodium chloride.

However, we could determine values for k_{on} with high accuracy only at ionic strengths of 0.04 M ($k_{on} = 9.4 \times 10^7$ M^{-1} s^{-1}) and 0.07 M ($k_{on} = 3.7 \times 10^7$ M^{-1} s^{-1}), because at higher salt concentrations the binding affinity becomes much weaker. Because of the poor quality of the stopped-flow traces at an ionic strength of 0.2 M, the k_{off} value could not be determined accurately but was estimated to be somewhere between 200 and 500 s^{-1} and a k_{on} of approximately $2-5 \times 10^6$ M^{-1} s^{-1}. The k_{off} appeared to have a weak dependence on ionic strength.

Interaction between NCBD and the PNT Domain. The PNT domain was included in the study as a folded protein ligand of NCBD. The kinetic traces obtained with the PNT domain (residues 60−170) were monophasic (Figure 3B), and the k_{obs} values increased linearly with NCBD concentration (Figure 3C). The k_{on} at a low ionic strength was much lower for the NCBD/PNT interaction than for the interaction between NCBD and the four disordered domains (Figure 4B and Table 1). Interestingly, the ionic strength dependence was found to be much weaker for the NCBD/PNT interaction (Figure 4B), indicating that the interaction between NCBD and the PNT domain relies on electrostatic interactions less than other NCBD interactions do. The k_{off} was 2.0 s^{-1} at an ionic strength of 0.2 M, which is similar to those of the other NCBD complexes except for p53TAD, with a 100-fold higher k_{off}. There is no three-dimensional structure available for the NCBD/PNT complex, but a previous study suggested that NCBD binds at the C-terminal part of the PNT domain.[15] We therefore determined the k_{off} for a longer construct of the PNT domain (from residue 60 to 195) and performed ITC measurements for three PNT variants of different lengths (60−170, 60−174, and 60−195) to determine the minimal length of the PNT domain that is required for binding to NCBD. The k_{off} of PNT(60−195) was found to be the same as that of the shorter PNT(60−170) variant, and all three PNT constructs bound to NCBD with the same K_d, within experimental error. We also performed binding measurements with PNT(76−170), truncated at the N-terminus, but judging from the ITC experiment, this variant displayed no binding to NCBD. Hence, The PNT domain, with a length that encompasses residues 60−170, contains the region that interacts with NCBD. Because the N- and C-terminal parts of the PNT domain are close to each other, both regions might be involved in the interaction with NCBD.

Interaction between NCBD and IRF-3. The IRF association domain of IRF-3 is another folded domain, which binds to NCBD and for which there is a crystal structure of the complex[16] (Figure 1). This interaction is particularly interesting because the crystal structure shows that NCBD binds IRF-3 in a distinct conformation, as compared to the complexes with SRC1,[32] ACTR,[17] and p53TAD.[13]

Using ITC, the K_d for the NCBD/IRF-3 interaction was determined to be around 100 μM at an ionic strength of 0.2 M (Figure 5C), thus, a lower affinity compared to those of the p160 co-activator domains but in the same range as for p53TAD. We also conducted stopped-flow studies at an ionic strength of 0.2 M, to investigate the binding kinetics, but could not observe a binding trace. The lack of trace is likely due to a combination of a relatively low affinity (resulting in a large k_{off} and thus a large observed rate constant) and a high total fluorescence of IRF-3 (giving a low signal-to-noise ratio).

Basal Rate Constants. Modulation of the ionic strength will affect electrostatic interactions.[27] In a recent study,[7] Clarke and co-workers determined the basal association rate constant,

DOI: 10.1021/acs.biochem.5b00520
Biochemistry 2015, 54, 4741−4750

Table 1. Rate Constants and K_d Values for NCBD Interactions, Determined in 10 mM MOPS (pH 7.4), at Different Ionic Strengths Adjusted with Sodium Chloride

binding partner	I (M)	k_{off} (s^{-1})	k_{on} (μM^{-1} s^{-1})	K_d (μM)	$k_{on,basal}$ (μM^{-1} s^{-1})
SRC1	0.044	1.3 ± 0.02	200 ± 20	0.006 ± 0.001	
	0.074	1.3 ± 0.001	105 ± 7	0.012 ± 0.001	
	0.20	1.5 ± 0.01	31 ± 1	0.047 ± 0.002	
	0.50	1.5 ± 0.04	14 ± 1	0.11 ± 0.01	
	1.00	1.2 ± 0.1	22 ± 3	0.053 ± 0.007	
					1.4 ± 1.2
TIF2	0.044	2.7 ± 0.3	350 ± 9	0.008 ± 0.001	
	0.074	2.9 ± 0.1	160 ± 4	0.018 ± 0.001	
	0.20	3.1 ± 0.02	58 ± 0.6	0.053 ± 0.001	
	0.50	2.3 ± 0.05	35 ± 2	0.066 ± 0.004	
	1.00	1.1 ± 0.01	24 ± 5	0.045 ± 0.010	
					2.0 ± 0.9
ACTR	0.044	2.1 ± 0.05	171 ± 6	0.012 ± 0.001	
	0.074	2.4 ± 0.02	91 ± 4	0.026 ± 0.001	
	0.20	2.7 ± 0.07	29 ± 0.4	0.094 ± 0.003	
	0.50	2.5 ± 0.03	18 ± 0.6	0.14 ± 0.005	
	1.00	1.4 ± 0.02	16 ± 2	0.086 ± 0.010	
					1.4 ± 0.8
p53TAD	0.044	280 ± 22	94 ± 14[b]	3.0 ± 0.4[a]	
	0.074	470 ± 90	37 ± 8[b]	13 ± 2[a]	
	0.20	~200−500	~2−5[b]	94 ± 0.6[a]	
	1.00	–	–	100 ± 6[a]	
					–
PNT	0.044	3.3 ± 0.03	7.1 ± 0.5	0.46 ± 0.03	
	0.074	2.6 ± 0.4	5.7 ± 0.4	0.46 ± 0.07	
	0.20	2.0 ± 0.1	3.5 ± 0.2	0.58 ± 0.04	
	0.50	1.8 ± 0.08	2.5 ± 0.1	0.71 ± 0.05	
	1.00	1.4 ± 0.05	1.9 ± 0.2	0.71 ± 0.07	
					0.57 ± 0.03
IRF-3	0.20			~100[a]	

[a]Determined by ITC. [b]Calculated ($k_{on} = k_{off}/K_d$) by combining ITC with the stopped-flow method. All measurements were taken at 277 K.

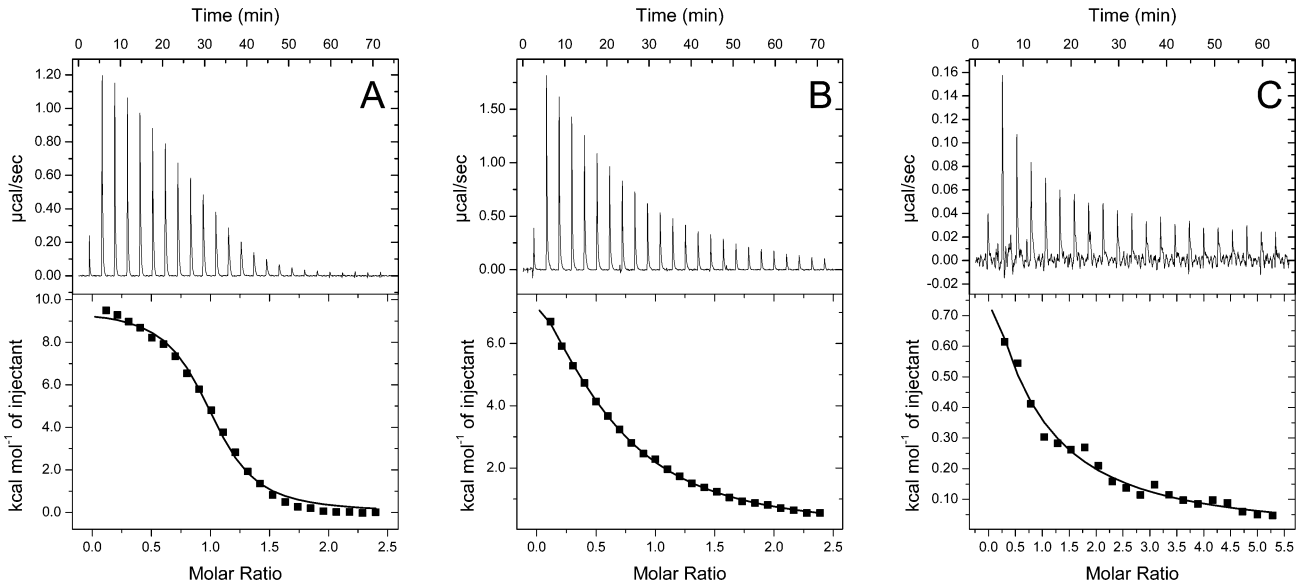

Figure 5. Equilibrium dissociation constants for NCBD/p53TAD and NCBD/IRF-3 determined using isothermal titration calorimetry at 277 K. (A) NCBD (0.86 mM) was titrated into 75 μM p53TAD at an ionic strength of 0.04 M. (B) NCBD (2.1 mM) was titrated into 190 μM p53TAD at an ionic strength of 0.2 M. (C) NCBD (1.4 mM) was titrated into 56 μM IRF-3 at an ionic strength of 0.2 M. See Table 1 for fitted K_d values.

$k_{on,basal}$, for the interaction between the disordered c-myb and the folded KIX domain and found that it was the highest reported to date for any protein−protein interaction. Using Debye−Hückel theory,[27] we calculated $k_{on,basal}$, at 277 K, for the interactions between NCBD and its protein ligands (Figure 6 and Table 1). Previously published $k_{on,basal}$ constants for other

DOI: 10.1021/acs.biochem.5b00520
Biochemistry 2015, 54, 4741−4750

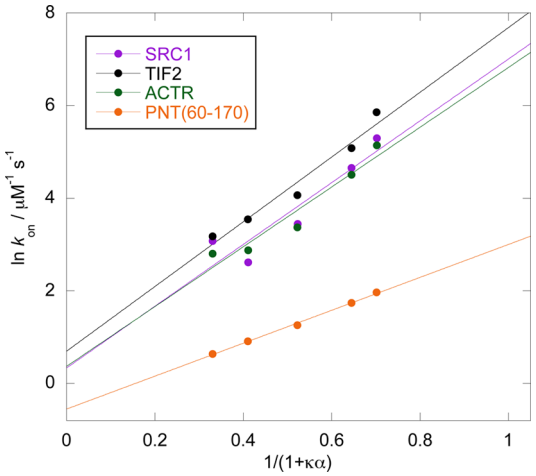

Figure 6. Basal association rate constant at 277 K determined from the ionic strength dependence of k_{on}, as the intercept with the *y*-axis (eq 1). The slope of the curve is $-U/RT$, where U is the electrostatic interaction energy. Buffer conditions were 10 mM MOPS (pH 7.4), with various sodium chloride concentrations.

protein−protein interactions have been determined mainly at 298 K (Shammas et al.[7] and references cited therein). Extrapolation of k_{on} from 277 and 283 K[21] for NCBD/ACTR to 298 K[22] results in a basal association rate constant of approximately 1−2 × 10^7 M^{-1} s^{-1} for the NCBD/ACTR interaction (and the other NCBD associations assuming a similar temperature dependence), similar to the value obtained for c-myb/KIX. Hence, our $k_{on,basal}$ values (Table 1) are also unusually high, exceeding the regime (10^4−10^6 M^{-1} s^{-1}) for diffusion-controlled reactions involving folded proteins.[27] We were not able to determine $k_{on,basal}$ for NCBD/p53TAD because of the very low binding affinity at ionic strengths equal to or higher than 0.2 M, which demanded increased protein concentrations, leading to a much higher total fluorescence that resulted in a low signal-to-noise ratio in the stopped-flow traces.

DISCUSSION

To fully understand the biological functions of IDPs, we must grasp their basic biophysical properties.[33] Further, we must relate these properties to those of globular proteins[34] to shed light on the question of whether there are fundamental differences between folded and disordered proteins. While IDPs have been the subject of intense theoretical and experimental research over the past 15 years, it is only recently that dedicated studies of the binding kinetics of IDPs have appeared.[7,8,21,22,24,35−41] Such studies are necessary to improve our understanding of the interplay between protein disorder and biological function[42] and in particular how different environmental conditions modulate the kinetics. They are also important for benchmarking computer simulations.[43−46] We have here investigated the binding of NCBD to a set of six different proteins, five of which were amenable to analysis of binding kinetics as a function of ionic strength.

It is clear that the interaction between NCBD and all four investigated disordered protein domains has a significant ionic strength dependence, which signifies the importance of electrostatic interactions for the formation of the complexes. Further, such dependence on the ionic strength implies that any local intracellular changes in salt concentration close to the physiological ionic strength could greatly affect the binding properties of IDPs. For instance, an increase in ionic strength from 0.074 to 0.20 M results in changes in K_d by 3−7-fold for the NCBD/IDP interactions.

In contrast to the strong salt dependence of the IDPs, the binding of NCBD to the folded PNT domain relies less on electrostatic interactions. This difference in electrostatic component is reflected in the 100-fold difference between the extrapolated k_{on} at zero ionic strength, i.e., at $1/(1 + \kappa\alpha) = 1$ in Figure 6 (k_{on} = 2 × 10^7 M^{-1} s^{-1} for PNT vs 0.9−2.2 × 10^9 M^{-1} s^{-1} for SRC1, TIF2, and ACTR). The reason for this difference may be found in the intriguing conformational changes of NCBD: the conformations that NCBD adopts when bound to SRC1, ACTR, and p53TAD are all very similar but are different from the IRF-3-bound structure (Figure 1). In the IRF-3-bound conformation,[16] most of the charged residues point away from IRF-3, resulting in a binding interface that relies more on hydrophobic interactions than that between NCBD and the three IDPs, SRC1, ACTR, and p53TAD. Furthermore, an NMR relaxation dispersion study demonstrated that within the unbound NCBD ensemble, a minor excited state that resembles the IRF-3-bound conformation is present.[20] Although one cannot say, at present, which structure NCBD adopts when it is complexed with the PNT domain, it is tempting to speculate that the PNT domain and IRF-3-bound NCBD conformations resemble each other. Future structural studies of NCBD/PNT will show whether NCBD utilizes a different conformation when interacting with proteins that rely less on electrostatic interactions, and the SRC1/ACTR/p53TAD-bound conformation when interacting with IDPs.

Four domains from CBP (TAZ1, TAZ2, KIX, and NCBD) are able to bind p53TAD, which contains two subdomains, AD1 and AD2.[12,47] Our p53TAD construct includes both AD1 and AD2. The NCBD/p53TAD structure reveals that NCBD interacts mainly with AD2,[13] which contains several acidic residues in the AD2 region that would make binding sensitive to changes in ionic strength. In fact, the K_d is increased by a factor of 31, going from 0.04 to 0.2 M in ionic strength (Figure 4C and Table 1). The k_{off} for NCBD/p53TAD is 2 orders of magnitude higher than those of the other complexes in this study, which might be due to greater residual disorder in the complex. For instance, NMR studies have demonstrated that several residues in p53TAD that interact with NCBD appear to be quite disordered,[13] with some of them not adopting regular secondary structures. This is to be compared with the NCBD/ACTR complex, which appears to have backbone dynamic properties typically observed for well-folded protein complexes.[28] Thus, residual disorder in the bound state could be a way for IDPs to modulate k_{off}, depending on the functional requirements.

It has been argued that IDPs in general have k_{off} values higher than those of folded proteins,[3,6] which could be advantageous when short-lived associations are desirable, such as in signaling. However, previous reports have shown that IDPs may display widely different k_{off} values, including very low ones, although, on average, there might exist a trend toward higher values.[5,6] In the study presented here, all of the NCBD/target complexes have relatively high k_{off} values compared to those of interactions involving folded proteins.[6] Assuming a similar temperature dependence[21,24] among NCBD complexes, estimated values at 298 K range from 15−30 s^{-1} (ACTR, SRC1, TIF2, and PNT domain) to 3000 s^{-1} (p53TAD). We can assume that the dissociation rate constant for NCBD/IRF-3 is also high,

DOI: 10.1021/acs.biochem.5b00520
Biochemistry 2015, 54, 4741−4750

because of the low binding affinity. Thus, the IDPs in our study form short-lived protein−protein complexes, lending support to the notion of a general trend in k_{off} between IDPs and folded proteins.[6] However, the variation in rate constants among available data sets is large,[5] and any general conclusions regarding both k_{off} and k_{on} must await further studies.

The association rate constant in the absence of electrostatic contributions, the basal association rate constant, $k_{on,basal}$, can be very informative from a mechanistic point of view. The association rate constant for two spherical particles that are uniformly reactive over their whole surface can be calculated using the Smoluchowski equation to be 10^9−10^{10} M^{-1} s^{-1}.[27] However, for proteins, such magnitudes are never reached because they are not uniformly reactive; for example, they usually have a binding site, which the ligand must enter in a certain conformation. Therefore, basal association rate constants for diffusion-controlled reactions involving folded proteins are around 10^4−10^6 M^{-1} s^{-1}.[27] The basal association rate constants determined in this study (0.57×10^6 M^{-1} s^{-1} for the folded PNT domain and 1.4−2.0×10^6 M^{-1} s^{-1} for the disordered p160 co-activator domains at 4 °C) are at the upper end of this regime or even exceeding it at 25 °C. One potential reason for this is that disordered proteins may be able to bind initially in several different ways; i.e., they have a significantly increased number of productive collisions leading to an encounter complex as compared to folded proteins. The initial complex for such IDP interactions may be very nonspecific and with non-native interactions, before rearrangement into the final native bound state.[48] This is consistent with a recent Φ value analysis of the interaction between ACTR and NCBD,[22] which showed that the transition state contains a few weak native hydrophobic contacts but is otherwise quite disordered. Similar arguments were put forward by Shammas et al.,[7] who also observed a high basal rate constant for the interaction between the disordered c-myb and the KIX domain, which the authors argued could be due to fewer obligatory contacts for the initial association.

A plausible model for the interaction between the full-length versions of p53 and CBP is a dimeric complex through a tetravalent interaction, in which each of the four p53TAD units binds to one of the four CBP domains, TAZ1, TAZ2, KIX, or NCBD.[12,47] The K_d for NCBD/p53TAD at a physiological ionic strength of 0.2 M is high, ∼90 μM, which would suggest that this interaction contributes little to the overall binding affinity of the tetramer. Previous studies[12] reported measurements of binding of p53TAD to NCBD, TAZ1, TAZ2, and KIX at a low ionic strength, making it difficult to assess the relative contribution each interaction makes to the overall binding affinity of CBP for p53 at a physiological ionic strength. The potentially different contribution of electrostatics for each individual interaction emphasizes the importance of conducting measurements at biologically relevant salt concentrations.

In conclusion, we have shown that IDP associations involving NCBD have high k_{on} values with a significant ionic strength dependence, which reflects the importance of electrostatic interactions in these interactions. On the other hand, the interaction between NCBD and the folded PNT domain depends less on electrostatic interactions, which may indicate a distinctly different interaction surface. Finally, the basal association rate constants determined in this study exceed those previously determined for folded proteins, suggesting that disordered proteins or regions initially associate with their targets in a manner less restricted than that of folded proteins.

■ ASSOCIATED CONTENT

Supporting Information

Biphasic binding trace for TIF2 at an ionic strength of 0.2 M (Figure S1A) and concentration dependence of the fast and slow kinetic phase for TIF2, at an ionic strength of 0.2 M (Figure S1B) and concentration dependence of the additional third kinetic phase that is observed at an ionic strength of 1 M (Figure S2). The Supporting Information is available free of charge on the ACS Publications website at DOI: 10.1021/acs.biochem.5b00520.

■ AUTHOR INFORMATION

Corresponding Authors

*E-mail: jakob.dogan@dbb.su.se.
*E-mail: Per.Jemth@imbim.uu.se. Phone: +46-18-4714557.

Present Address

†J.D.: Department of Biochemistry and Biophysics, Stockholm University, SE-10691 Stockholm, Sweden.

Funding

This work was supported by the Swedish Research Council (NT) and the Human Frontiers Young Investigator Science Program (to P.J.), and by the Magnus Bergvall Foundation, Lars Hierta Memorial Foundation, and the O. E. and EDLA Johansson's Scientific Foundation (to J.D.).

Notes

The authors declare no competing financial interest.

■ ABBREVIATIONS

ACTR, activator for thyroid hormone and retinoid receptors; CBP, CREB binding protein; CREB, cAMP response element binding; DTT, dithiothreitol; IDP, intrinsically disordered protein; IDR, intrinsically disordered region; IRF-3, interferon regulatory factor-3; NCOA, p160 nuclear co-activator; p53TAD, p53 transactivation domain; PDB, Protein Data Bank; PNT, pointed domain; SRC1, steroid receptor co-activator 1; TCEP, Tris(2-carboxyethyl)phosphine; TIF2, transcriptional intermediatory factor 2.

■ REFERENCES

(1) Wright, P. E., and Dyson, H. J. (2015) Intrinsically disordered proteins in cellular signalling and regulation. *Nat. Rev. Mol. Cell Biol. 16*, 18−29.

(2) Uversky, V. N., Oldfield, C. J., and Dunker, A. K. (2008) Intrinsically disordered proteins in human diseases: introducing the D2 concept. *Annu. Rev. Biophys. 37*, 215−246.

(3) Zhou, H.-X. (2012) Intrinsic disorder: signaling via highly specific but short-lived association. *Trends Biochem. Sci. 37*, 43−48.

(4) Uversky, V. N., Gillespie, J. R., and Fink, A. L. (2000) Why are "natively unfolded" proteins unstructured under physiologic conditions? *Proteins: Struct., Funct., Genet. 41*, 415−427.

(5) Dogan, J., Gianni, S., and Jemth, P. (2014) The binding mechanisms of intrinsically disordered proteins. *Phys. Chem. Chem. Phys. 16*, 6323−6331.

(6) Shammas, S. L., Rogers, J. M., Hill, S. A., and Clarke, J. (2012) Slow, reversible, coupled folding and binding of the spectrin tetramerization domain. *Biophys. J. 103*, 2203−2214.

(7) Shammas, S. L., Travis, A. J., and Clarke, J. (2013) Remarkably fast coupled folding and binding of the intrinsically disordered transactivation domain of cMyb to CBP KIX. *J. Phys. Chem. B 117*, 13346−13356.

(8) Rogers, J. M., Steward, A., and Clarke, J. (2013) Folding and binding of an intrinsically disordered protein: fast, but not "diffusion-limited. *J. Am. Chem. Soc. 135*, 1415−1422.

DOI: 10.1021/acs.biochem.5b00520
Biochemistry 2015, 54, 4741−4750

(9) Huang, Y., and Liu, Z. (2009) Kinetic advantage of intrinsically disordered proteins in coupled folding-binding process: a critical assessment of the "fly-casting" mechanism. *J. Mol. Biol. 393*, 1143−1159.
(10) Wang, F., Marshall, C. B., and Ikura, M. (2013) Transcriptional/epigenetic regulator CBP/p300 in tumorigenesis: structural and functional versatility in target recognition. *Cell. Mol. Life Sci. 70*, 3989−4008.
(11) Xu, J., and Li, Q. (2003) Review of the in vivo functions of the p160 steroid receptor coactivator family. *Mol. Endocrinol. 17*, 1681−1692.
(12) Ferreon, J. C., Lee, C. W., Arai, M., Martinez-Yamout, M. A., Dyson, H. J., and Wright, P. E. (2009) Cooperative regulation of p53 by modulation of ternary complex formation with CBP/p300 and HDM2. *Proc. Natl. Acad. Sci. U. S. A. 106*, 6591−6596.
(13) Lee, C. W., Martinez-Yamout, M. A., Dyson, H. J., and Wright, P. E. (2010) Structure of the p53 transactivation domain in complex with the nuclear receptor coactivator binding domain of CREB binding protein. *Biochemistry 49*, 9964−9971.
(14) Lin, C. H., Hare, B. J., Wagner, G., Harrison, S. C., Maniatis, T., and Fraenkel, E. (2001) A small domain of CBP/p300 binds diverse proteins: solution structure and functional studies. *Mol. Cell 8*, 581−590.
(15) Matsuda, S., Harries, J. C., Viskaduraki, M., Troke, P. J. F., Kindle, K. B., Ryan, C., and Heery, D. M. (2004) A Conserved alpha-helical motif mediates the binding of diverse nuclear proteins to the SRC1 interaction domain of CBP. *J. Biol. Chem. 279*, 14055−14064.
(16) Qin, B. Y., Liu, C., Srinath, H., Lam, S. S., Correia, J. J., Derynck, R., and Lin, K. (2005) Crystal structure of IRF-3 in complex with CBP. *Structure 13*, 1269−1277.
(17) Demarest, S. J., Martinez-Yamout, M., Chung, J., Chen, H., Xu, W., Dyson, H. J., Evans, R. M., and Wright, P. E. (2002) Mutual synergistic folding in recruitment of CBP/p300 by p160 nuclear receptor coactivators. *Nature 415*, 549−553.
(18) Demarest, S. J., Deechongkit, S., Dyson, H. J., Evans, R. M., and Wright, P. E. (2004) Packing, specificity, and mutability at the binding interface between the p160 coactivator and CREB-binding protein. *Protein Sci. 13*, 203−210.
(19) Kjaergaard, M., Teilum, K., and Poulsen, F. M. (2010) Conformational selection in the molten globule state of the nuclear coactivator binding domain of CBP. *Proc. Natl. Acad. Sci. U. S. A. 107*, 12535−12540.
(20) Kjaergaard, M., Andersen, L., Nielsen, L. D., and Teilum, K. (2013) A folded excited state of ligand-free nuclear coactivator binding domain (NCBD) underlies plasticity in ligand recognition. *Biochemistry 52*, 1686−1693.
(21) Dogan, J., Schmidt, T., Mu, X., Engström, Å., and Jemth, P. (2012) Fast association and slow transitions in the interaction between two intrinsically disordered protein domains. *J. Biol. Chem. 287*, 34316−34324.
(22) Dogan, J., Mu, X., Engström, Å., and Jemth, P. (2013) The transition state structure for coupled binding and folding of disordered protein domains. *Sci. Rep. 3*, 2076.
(23) Iešmantavičius, V., Dogan, J., Jemth, P., Teilum, K., and Kjaergaard, M. (2014) Helical propensity in an intrinsically disordered protein accelerates ligand binding. *Angew. Chem., Int. Ed. 53*, 1548−1551.
(24) Jemth, P., Mu, X., Engström, Å., and Dogan, J. (2014) A frustrated binding interface for intrinsically disordered proteins. *J. Biol. Chem. 289*, 5528−5533.
(25) Malatesta, F. (2005) The study of bimolecular reactions under non-pseudo-first order conditions. *Biophys. Chem. 116*, 251−256.
(26) Fersht, A. (1999) *Structure and mechanism in protein science: A guide to enzyme catalysis and protein folding*, Macmillan, New York.
(27) Schreiber, G., Haran, G., and Zhou, H.-X. (2009) Fundamental aspects of protein-protein association kinetics. *Chem. Rev. 109*, 839−860.
(28) Ebert, M.-O., Bae, S.-H., Dyson, H. J., and Wright, P. E. (2008) NMR relaxation study of the complex formed between CBP and the activation domain of the nuclear hormone receptor coactivator ACTR. *Biochemistry 47*, 1299−1308.
(29) Kjaergaard, M., Nørholm, A.-B., Hendus-Altenburger, R., Pedersen, S. F., Poulsen, F. M., and Kragelund, B. B. (2010) Temperature-dependent structural changes in intrinsically disordered proteins: formation of alpha-helices or loss of polyproline II? *Protein Sci. 19*, 1555−1564.
(30) Lee, H., Mok, K. H., Muhandiram, R., Park, K. H., Suk, J. E., Kim, D. H., Chang, J., Sung, Y. C., Choi, K. Y., and Han, K. H. (2000) Local structural elements in the mostly unstructured transcriptional activation domain of human p53. *J. Biol. Chem. 275*, 29426−29432.
(31) Wells, M., Tidow, H., Rutherford, T. J., Markwick, P., Jensen, M. R., Mylonas, E., Svergun, D. I., Blackledge, M., and Fersht, A. R. (2008) Structure of tumor suppressor p53 and its intrinsically disordered N-terminal transactivation domain. *Proc. Natl. Acad. Sci. U. S. A. 105*, 5762−5767.
(32) Waters, L., Yue, B., Veverka, V., Renshaw, P., Bramham, J., Matsuda, S., Frenkiel, T., Kelly, G., Muskett, F., Carr, M., and Heery, D. M. (2006) Structural diversity in p160/CREB-binding protein coactivator complexes. *J. Biol. Chem. 281*, 14787−14795.
(33) Uversky, V. N. (2013) A decade and a half of protein intrinsic disorder: biology still waits for physics. *Protein Sci. 22*, 693−724.
(34) Schreiber, G. (2002) Kinetic studies of protein−protein interactions. *Curr. Opin. Struct. Biol. 12*, 41−47.
(35) Bachmann, A., Wildemann, D., Praetorius, F., Fischer, G., and Kiefhaber, T. (2011) Mapping backbone and side-chain interactions in the transition state of a coupled protein folding and binding reaction. *Proc. Natl. Acad. Sci. U. S. A. 108*, 3952−3957.
(36) Haq, S. R., Chi, C. N., Bach, A., Dogan, J., Engström, Å., Hultqvist, G., Karlsson, O. A., Lundström, P., Montemiglio, L. C., Strømgaard, K., Gianni, S., and Jemth, P. (2012) Side-chain interactions form late and cooperatively in the binding reaction between disordered peptides and PDZ domains. *J. Am. Chem. Soc. 134*, 599−605.
(37) Karlsson, O. A., Chi, C. N., Engström, A., and Jemth, P. (2012) The transition state of coupled folding and binding for a flexible *β*-finger. *J. Mol. Biol. 417*, 253−261.
(38) Gianni, S., Morrone, A., Giri, R., and Brunori, M. (2012) A folding-after-binding mechanism describes the recognition between the transactivation domain of c-Myb and the KIX domain of the CREB-binding protein. *Biochem. Biophys. Res. Commun. 428*, 205−209.
(39) Toto, A., Giri, R., Brunori, M., and Gianni, S. (2014) The mechanism of binding of the KIX domain to the mixed lineage leukemia protein and its allosteric role in the recognition of c-Myb. *Protein Sci. 23*, 962−969.
(40) Dosnon, M., Bonetti, D., Morrone, A., Erales, J., di Silvio, E., Longhi, S., and Gianni, S. (2015) Demonstration of a Folding after Binding Mechanism in the Recognition between the Measles Virus NTAIL and X Domains. *ACS Chem. Biol. 10*, 795−802.
(41) Rogers, J. M., Wong, C. T., and Clarke, J. (2014) Coupled Folding and Binding of the Disordered Protein PUMA Does Not Require Particular Residual Structure. *J. Am. Chem. Soc. 136*, 5197−5200.
(42) Gibbs, E. B., and Showalter, S. A. (2015) Quantitative biophysical characterization of intrinsically disordered proteins. *Biochemistry 54*, 1314−1326.
(43) Zhou, H.-X., Pang, X., and Lu, C. (2012) Rate constants and mechanisms of intrinsically disordered proteins binding to structured targets. *Phys. Chem. Chem. Phys. 14*, 10466−10476.
(44) Ganguly, D., Otieno, S., Waddell, B., Iconaru, L., Kriwacki, R. W., and Chen, J. (2012) Electrostatically accelerated coupled binding and folding of intrinsically disordered proteins. *J. Mol. Biol. 422*, 674−684.
(45) Ganguly, D., Zhang, W., and Chen, J. (2013) Electrostatically accelerated encounter and folding for facile recognition of intrinsically disordered proteins. *PLoS Comput. Biol. 9*, e1003363.
(46) Knott, M., and Best, R. B. (2014) Discriminating binding mechanisms of an intrinsically disordered protein via a multi-state coarse-grained model. *J. Chem. Phys. 140*, 175102.

DOI: 10.1021/acs.biochem.5b00520
Biochemistry 2015, 54, 4741−4750

(47) Teufel, D. P., Freund, S. M., Bycroft, M., and Fersht, A. R. (2007) Four domains of p300 each bind tightly to a sequence spanning both transactivation subdomains of p53. *Proc. Natl. Acad. Sci. U. S. A. 104*, 7009−7014.
(48) Blöchliger, N., Xu, M., and Caflisch, A. (2015) Peptide Binding to a PDZ Domain by Electrostatic Steering via Nonnative Salt Bridges. *Biophys. J. 108*, 2362−2370.

DOI: 10.1021/acs.biochem.5b00520
Biochemistry 2015, 54, 4741−4750